A Decentralized Approach to Formation Maneuvers

Jonathan R. T. Lawton, Randal W. Beard, *Senior Member, IEEE*, and Brett J. Young

***Abstract*—This paper presents a behavior-based approach to formation maneuvers for groups of mobile robots. Complex formation maneuvers are decomposed into a sequence of maneuvers between formation patterns. The paper presents three formation control strategies. The first strategy uses relative position information configured in a bidirectional ring topology to maintain the formation. The second strategy injects interrobot damping via passivity techniques. The third strategy accounts for actuator saturation. Hardware results demonstrate the effectiveness of the proposed control strategies.**

***Index Terms*—Behavioral methods, coordinated control, formations, mobile robots, passivity.**

I. Introduction

COOPERATIVE robots can be used to perform tasks that are too difficult for a single robot to perform alone. For example, a group of robots can be used to move large awkward objects [1], [2], or to move a large number of objects [3]. In addition, groups of robots can be used for terrain model acquisition [3], planetary exploration [4], or measuring radiation levels over a large area [5]. In [6], a group of robots are used for path obstruction. This could be used to impede the motion of an intruder in a battlefield scenario.

There are roughly three approaches to multivehicle coordination reported in the literature: leader following; behavioral methods; and virtual structure techniques. In leader following, some robots are designated as leaders, while others are designated as followers [7]–[10]. In behavior-based control [11]–[16], several desired behaviors are prescribed for each agent, and the final control is derived from a weighting of the relative importance of each behavior. In the virtual structure approach, the entire formation is treated as a single entity [17]–[20]. Desired motion is assigned to the virtual structure which traces out trajectories for each member of the formation to follow.

The virtual structure and leader-following approaches require that the full state of the leader or virtual structure be communicated to each member of the formation. However, behavior-based approaches are decentralized and may be implemented with significantly less communication. The disadvantage of behavior-based approaches is that they are difficult to analyze mathematically. Therefore, it is difficult to guarantee that the formation has converged to the desired configuration, or to guarantee formation keeping during a maneuver.

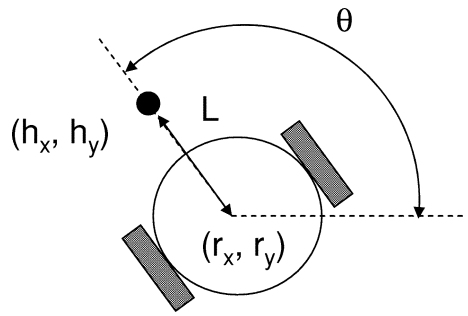

Fig. 1. Nonholonomic differentially driven mobile robot.

In this paper, we will consider three behavioral control strategies. Hardware results will be presented, demonstrating the effectiveness of the approach on differentially driven mobile robots. The position of each robot is measured using a combination of dead reckoning and an overhead camera system. The fact that we use differentially driven mobile robots complicates the coordination problem, due to the nonholonomic constraints. In the well-known paper by Brockett [21], it was shown that nonholonomic systems cannot be stabilized with continuous static state feedback. The implication for differential-drive mobile robots is that the position and orientation of the center of the robot cannot be simultaneously stabilized with a time-invariant, stabilizing control strategy. Both discontinuous control laws [22], [23] and time-varying [24], [25] control laws have been found to stabilize the center of rotation and the orientation of a single robot. The multiple robot case is naturally more complex.

Define the "hand" position of the robot to be the point $\mathbf{h} = (h_x, h_y)$ that lies a distance L along the line that is normal to the wheel axis and intersects the wheel axis at the center point $\mathbf{r} = (r_x, r_y)$, as shown in Fig. 1. The kinematics of the hand position are holonomic for $L \neq 0$. In this paper, we consider the problem of coordinating the hand position of the robots. While this assumption simplifies the control problem, it is of importance since the hand position may, in fact, be the point of interest. For example, if the robots are equipped with a gripper located at the hand position and the coordination task is to move an object from one location to another, then the objective is to move the gripper locations in a coordinated fashion. Another example is when the group objective is the coordinated placement of sensors that are located at the hand position.

Manuscript received September 23, 1999; revised June 18, 2001. This paper was recommended for publication by Associate Editor J.-P. Laumond and Editor S. Salcudean upon evaluation of the reviewers' comments. This work was supported by the Jet Propulsion Laboratory, California Institute of Technology, Pasadena, CA, under Contract 96-1245. The work of J. R. T. Lawton was supported in part by a Rocky Mountain NASA Space Grant Consortium Fellowship. This paper was presented in part at the IEEE International Conference on Robotics and Automation, San Francisco, CA, April 2000.

J. R. T. Lawton and B. J. Young are with Raytheon Missile Systems, Tucson, AZ 85706 USA (e-mail: jonathan_r_lawton@raytheon.com; brett_j_young@raytheon.com).

R. W. Beard is with the Electrical and Computer Engineering Department, Brigham Young University, Provo, UT 84602 USA (e-mail: beard@ee.byu.edu).

Digital Object Identifier 10.1109/TRA.2003.819598

The objective of this paper is to introduce the coupled dynamics approach to formation control, which is a behavior-based strategy. The paper provides a rigorous analysis of formation keeping and convergence, which is a contribution to the behavior-based literature. Furthermore, our approach has the advantage that it can be implemented when only neighbor position information is available (i.e., velocity information is not required), thereby reducing the communication overhead.

In Section II, we derive the equations of motion for the hand position and show that the internal dynamics are stable in the sense of Lyapunov. In Section III, we define the formation control problem as motion between a sequence of formation patterns. In Section IV, we present three coupled dynamics control strategies. The first strategy uses the global and relative position of each robot to move the robot formation from one position to another while maintaining the robots in formation during the maneuver. In the absence of relative velocity information, the relative motion among robots can be oscillatory when controlled by the coupled dynamics approach. The second control strategy introduces passivity-based interrobot damping to significantly reduce interrobot oscillations. The third strategy considers formation control subject to robot actuator constraints. Section V presents hardware results for each of these control strategies, and Section VI offers some concluding remarks.

II. Robot Dynamics

The objective of this paper is formation control for a group of mobile robots, each of which have the following equations of motion:

$$\begin{pmatrix} \dot{r}_{xi} \\ \dot{r}_{yi} \\ \dot{\theta}_i \\ \dot{v}_i \\ \dot{\omega}_i \end{pmatrix} = \begin{pmatrix} v_i \cos(\theta_i) \\ v_i \sin(\theta_i) \\ \omega_i \\ 0 \\ 0 \end{pmatrix} + \begin{pmatrix} 0 & 0 \\ 0 & 0 \\ 0 & 0 \\ \frac{1}{m_i} & 0 \\ 0 & \frac{1}{J_i} \end{pmatrix} \begin{pmatrix} F_i \\ \tau_i \end{pmatrix} \quad (1)$$

where $\mathbf{r}_i = (r_{xi}, r_{yi})^T$ is the inertial position of the ith robot, θ_i is the orientation, v_i is the linear speed, ω_i is the angular speed, τ_i is the applied torque, F_i is the applied force, m_i is the mass, and J_i is the moment of inertia. Letting $\mathbf{x}_i = (r_{xi}, r_{yi}, \theta_i, v_i, \omega_i)^T$, and $\mathbf{u}_i = (F_i, \tau_i)^T$, the equations of motion can be written as

$$\mathbf{x}_i = f(\mathbf{x}_i) + g_i \mathbf{u}_i \quad (2)$$

where the definitions of f and g_i can be inferred from (1).

In this paper, we will focus on formation control of the robot hand position. As shown in Fig. 1, the hand position is a point located a distance L_i along the line that is perpendicular to the wheel axis and intersects $\mathbf{r}_i$. The hand position is given by the equations

$$\mathbf{h}_i = \mathbf{r}_i + L_i \begin{pmatrix} \cos(\theta_i) \\ \sin(\theta_i) \end{pmatrix}. \quad (3)$$

Differentiating (3) with respect to time gives

$$\dot{\mathbf{h}}_i = \begin{pmatrix} \cos(\theta_i) & -L_i \sin(\theta_i) \\ \sin(\theta_i) & L_i \cos(\theta_i) \end{pmatrix} \begin{pmatrix} v_i \\ \omega_i \end{pmatrix}.$$

Differentiating again gives

$$\ddot{\mathbf{h}}_i = \begin{pmatrix} -v_i\omega_i \sin(\theta_i) - L_i\omega_i^2 \cos(\theta_i) \\ v_i\omega_i \cos(\theta_i) - L_i\omega_i^2 \sin(\theta_i) \end{pmatrix} + \begin{pmatrix} \frac{1}{m_i}\cos(\theta_i) & -\frac{L_i}{J_i}\sin(\theta_i) \\ \frac{1}{m_i}\sin(\theta_i) & \frac{L_i}{J_i}\cos(\theta_i) \end{pmatrix} \begin{pmatrix} F_i \\ \tau_i \end{pmatrix}.$$

Since

$$\det \begin{pmatrix} \frac{1}{m_i}\cos(\theta_i) & -\frac{L_i}{J_i}\sin(\theta_i) \\ \frac{1}{m_i}\sin(\theta_i) & \frac{L_i}{J_i}\cos(\theta_i) \end{pmatrix} = \frac{L_i}{m_i J_i} \neq 0$$

the system (2) with output (3) has constant relative degree equal to two and can, therefore, be output feedback linearized [26] about the hand position. Toward that end, define the map $\psi : \mathbb{R}^5 \to \mathbb{R}^5$ as

$$\boldsymbol{\zeta}_i = \psi(\mathbf{x}_i) \triangleq \begin{pmatrix} r_{xi} + L_i \cos(\theta_i) \\ r_{yi} + L_i \sin(\theta_i) \\ v_i \cos(\theta_i) - L_i \omega_i \sin(\theta_i) \\ v_i \sin(\theta_i) + L_i \omega_i \cos(\theta_i) \\ \theta_i \end{pmatrix}. \quad (4)$$

The map ψ is a diffeomorphism, and its inverse is given by

$$\mathbf{x}_i = \psi^{-1}(\boldsymbol{\zeta}_i) = \begin{pmatrix} \zeta_{1i} - L_i \cos(\zeta_{5i}) \\ \zeta_{2i} - L_i \sin(\zeta_{5i}) \\ \zeta_{5i} \\ \frac{1}{2}\zeta_{3i}\cos(\zeta_{5i}) + \frac{1}{2}\zeta_{4i}\sin(\zeta_{5i}) \\ -\frac{1}{2L_i}\zeta_{3i}\sin(\zeta_{5i}) + \frac{1}{2L_i}\zeta_{4i}\cos(\zeta_{5i}) \end{pmatrix}.$$

In the transformed coordinates, (2) and (3) are given by

$$\begin{aligned} \begin{pmatrix} \dot{\zeta}_{1i} \\ \dot{\zeta}_{2i} \end{pmatrix} &= \begin{pmatrix} \zeta_{3i} \\ \zeta_{4i} \end{pmatrix} \\ \begin{pmatrix} \dot{\zeta}_{3i} \\ \dot{\zeta}_{4i} \end{pmatrix} &= \begin{pmatrix} -v_i\omega_i \sin(\theta_i) - L_i\omega_i^2 \cos(\theta_i) \\ v_i\omega_i \cos(\theta_i) - L_i\omega_i^2 \sin(\theta_i) \end{pmatrix} \\ &\quad + \begin{pmatrix} \frac{1}{m_i}\cos(\theta_i) & -\frac{L_i}{J_i}\sin(\theta_i) \\ \frac{1}{m_i}\sin(\theta_i) & \frac{L_i}{J_i}\cos(\theta_i) \end{pmatrix} \mathbf{u}_i \\ \dot{\zeta}_{5i} &= -\frac{1}{2L_i}\zeta_{3i}\sin(\zeta_{5i}) + \frac{1}{2L_i}\zeta_{4i}\cos(\zeta_{5i}). \end{aligned}$$

The output feedback linearizing control [26] is given by

$$\mathbf{u}_i = \begin{pmatrix} \frac{1}{m_i}\cos(\theta_i) & -\frac{L_i}{J_i}\sin(\theta_i) \\ \frac{1}{m_i}\sin(\theta_i) & \frac{L_i}{J_i}\cos(\theta_i) \end{pmatrix}^{-1} \times \left[\boldsymbol{\nu}_i - \begin{pmatrix} -v_i\omega_i \sin(\theta_i) - L_i\omega_i^2 \cos(\theta_i) \\ v_i\omega_i \cos(\theta_i) - L_i\omega_i^2 \sin(\theta_i) \end{pmatrix} \right] \quad (5)$$

which gives

$$\begin{aligned} \begin{pmatrix} \dot{\zeta}_{1i} \\ \dot{\zeta}_{2i} \end{pmatrix} &= \begin{pmatrix} \zeta_{3i} \\ \zeta_{4i} \end{pmatrix} \\ \begin{pmatrix} \dot{\zeta}_{3i} \\ \dot{\zeta}_{4i} \end{pmatrix} &= \boldsymbol{\nu}_i \\ \dot{\zeta}_{5i} &= -\frac{1}{2L_i}\zeta_{3i}\sin(\zeta_{5i}) + \frac{1}{2L_i}\zeta_{4i}\cos(\zeta_{5i}) \\ \mathbf{h}_i &= \begin{pmatrix} \zeta_{1i} \\ \zeta_{2i} \end{pmatrix}. \end{aligned}$$

The last equation represents the internal dynamics which are rendered unobservable and uncontrollable by the transformation (4). The zero dynamics [26] are found by setting $\zeta_{1i} = \cdots =$

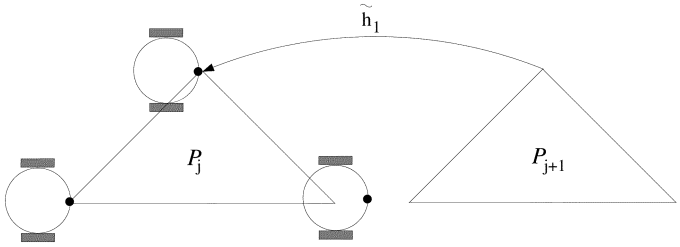

Fig. 2. Bottom right member of the formation is initially too far to the right.

$\zeta_{4i} = 0$ to get $\dot{\zeta}_{5i} = 0$. Therefore, the zero dynamics are stable, but not asymptotically stable. Since $\zeta_{5i} = \theta_i$ and $(\zeta_{3i}, \zeta_{4i})^T$ represent the velocity of the hand position, this implies that the angle θ_i will stop moving when the hand position stops moving.

In the remainder of the paper, the input–output dynamics of each robot will be represented by the double integrator system

$$\ddot{\mathbf{h}}_i = \boldsymbol{\nu}_i. \tag{6}$$

Feedback linearization about the hand position was used in [25] for kinematic models. This section has extended the approach to dynamic models, and has explicitly defined the internal dynamics.

III. Formation Maneuvers

In this section, we describe the types of formation maneuvers that will be considered in this paper. Let N be the number of mobile robots in the formation. A *formation pattern* is defined to be a set

$$\mathcal{P} = \{\mathbf{h}_1^d, \ldots, \mathbf{h}_N^d\}$$

where $\mathbf{h}_i^d$ is the desired location of the hand position of the ith robot. We will consider the class of formation control problems where the group of robots is required to transition through a sequence of formation patterns $\mathcal{P}_j, j = 1, \ldots, J$, where we assume that the sequence of formation patterns are designed in such a way as to avoid robot collisions. We assume that during the transition from one formation pattern to another, it is desirable to maintain the robots in the same shape as the destination pattern.

There are two competing objectives. The first objective is to move the robots to their final destination as specified in the formation pattern. The second objective is to maintain formation during the transition. Consider a simple translation as shown in Fig. 2. The left triangle represents the formation pattern at the start of the maneuver, and the right triangle represents the desired formation pattern. Suppose that initially the bottom right robot leads the formation, as shown in Fig. 2. The robot has two conflicting objectives: move right to arrive at the final goal, and move left to regain formation. If it moves left it will likely overshoot the formation, which is moving to the right, and if it moves right, it will take longer to regain formation as the others are required to catch up.

To incorporate these two competing objectives, we will define error functions for both. Let E_g be the total error between the current position of the robots and the desired formation pattern

$$E_g = \sum_{i=1}^{N} \tilde{\mathbf{h}}_i^T K_g \tilde{\mathbf{h}}_i$$

where K_g is a symmetric positive definite matrix, and $\tilde{\mathbf{h}}_i = \mathbf{h}_i - \mathbf{h}_i^d$ (see Fig. 2). Similarly, define E_f as the formation error

$$E_f = \sum_{i=\langle N \rangle} (\tilde{\mathbf{h}}_i - \tilde{\mathbf{h}}_{i+1})^T K_f (\tilde{\mathbf{h}}_i - \tilde{\mathbf{h}}_{i+1})$$

where $K_f = K_f^T \geq 0$, and where the robot index is defined modulo N, i.e., $\tilde{\mathbf{h}}_{N+1} = \tilde{\mathbf{h}}_1$, and $\tilde{\mathbf{h}}_0 = \tilde{\mathbf{h}}_N$. The notation $i = \langle N \rangle$ is used to indicate summation around the ring defined by the formation pattern. By maintaining E_f small during the maneuver, the robots will equalize the distance that they need to go to reach the final formation pattern. Note that $E_f = 0$ if and only if $\tilde{\mathbf{h}}_i = \tilde{\mathbf{h}}_{i+1}$ for all i. This is equivalent to saying that $\mathbf{h}_i - \mathbf{h}_{i+1} = \mathbf{h}_i^d - \mathbf{h}_{i+1}^d$, which will only be true if the robots are in the same relative formation that they will have at the end of the maneuver. Therefore, when $E_f = 0$, the robots will be keeping formation, but they will not necessarily be at the final formation pattern.

The total error for the formation coordination problem is the sum of E_g and E_f

$$\begin{aligned} E(t) &= E_f(t) + E_g(t) \\ &= \sum_{i=\langle N \rangle} \left[\tilde{\mathbf{h}}_i^T K_g \tilde{\mathbf{h}}_i + (\tilde{\mathbf{h}}_i - \tilde{\mathbf{h}}_{i+1})^T K_f (\tilde{\mathbf{h}}_i - \tilde{\mathbf{h}}_{i+1}) \right] \end{aligned} \tag{7}$$

where K_f and K_g weight the relative importance of formation keeping versus goal convergence. The formation control objective is to drive $E \to 0$ asymptotically.

IV. Formation Control

In this section, we propose three control strategies for driving $E(t)$ defined in (7) to zero, given the dynamics (6). The first approach is the *coupled dynamics formation control* derived in Section IV-A. The coupled dynamics approach couples the dynamics of the robots by incorporating relative position and velocity information between neighbors in the control strategy. This approach requires that each robot knows the relative position and velocity of two other robots (its neighbors in the communication ring), as well as their desired positions in the target formation pattern. The second approach, derived in Section IV-B, is the *coupled dynamics formation control with passivity-based interrobot damping*. This formation control strategy is identical to the coupled dynamics approach, except the requirement for relative velocity is removed. The third approach, derived in Section IV-C, is the *coupled dynamics approach with saturated control*. This strategy modifies the

coupled dynamics approach so that convergence of E is guaranteed under actuator saturation constraints.

A. Coupled Dynamics Formation Control

In this section, we derive the coupled dynamics formation control strategy. The proposed control law is given by

$$\begin{aligned}\boldsymbol{\nu}_i = &-K_g\tilde{\mathbf{h}}_i - D_g\dot{\mathbf{h}}_i \\ &- K_f(\tilde{\mathbf{h}}_i - \tilde{\mathbf{h}}_{i-1}) - D_f(\dot{\mathbf{h}}_i - \dot{\mathbf{h}}_{i-1}) \\ &- K_f(\tilde{\mathbf{h}}_i - \tilde{\mathbf{h}}_{i+1}) - D_f(\dot{\mathbf{h}}_i - \dot{\mathbf{h}}_{i+1}) \end{aligned} \tag{8}$$

where K_f and D_f are symmetric positive semidefinite matrices, and K_g and D_g are symmetric positive definite.

The first two terms in (8) drive the robot to its final position in the formation pattern. The second two terms maintain formation with the $i-1$ robot, and the last two terms maintain formation with the $i+1$ robot.

Theorem IV.1: If the robot formation (1) is subject to the control strategy defined in (5) and (8), then the error function (7) converges to zero asymptotically.

Furthermore, if the formation is initially at rest, i.e., $\dot{\mathbf{h}}(0) = 0$, then the formation error is bounded by

$$E(t) \leq E(0) - \sum_{i=1}^{N} \dot{\mathbf{h}}_i^T \dot{\mathbf{h}}_i. \tag{9}$$

The proof of this theorem and *Theorem IV.2* are simplified by the use of Kronecker product notation [27]. The following Lemma serves to establish our notation and makes the derivations in the proofs of *Theorems IV.1* and *IV.2* more transparent.

Lemma IV.1: Let C be the Hankel matrix defined by the row vector

$$(2, -1, 0, \ldots, 0, -1) \in \mathbb{R}^N$$

then $C \in \mathbb{R}^{N\times N}$ is symmetric positive definite. If $\boldsymbol{\xi} = (\xi_1^T, \ldots, \xi_N^T)^T$ where $\xi_i \in \mathbb{R}^p$, then

$$\sum_{i=\langle N\rangle} (\xi_i - \xi_{i+1})^T J(\xi_i - \xi_{i+1}) = \boldsymbol{\xi}^T (C \otimes J)\boldsymbol{\xi}$$

where $\otimes$ denotes the Kronecker product of two matrices. If the terms $J(\xi_i - \xi_{i-1}) + J(\xi_i - \xi_{i+1})$ are stacked in a column vector, the resulting vector can be written as $(C \otimes J)\boldsymbol{\xi}$. In addition, if $J \in \mathbb{R}^{p\times p}$ is positive definite, then $(C \otimes J) \in \mathbb{R}^{Np\times Np}$ is positive definite.

Proof: By direct substitution, it can be verified that the matrix C can be factored as $C = \hat{C}^T\hat{C}$, where $\hat{C} = [\hat{c}_{ij}]$ is defined by

$$\hat{c}_{ij} = \begin{cases} 1, & j = i \\ -1, & j = i + 1 (\mathrm{mod}\, N) \\ 0, & \text{otherwise.} \end{cases} \tag{10}$$

It is clear that $\hat{C}$ is full rank, therefore, C is symmetric and positive definite.

The second fact is verified as follows:

$$\begin{aligned}\boldsymbol{\xi}^T(C \otimes J)\boldsymbol{\xi} &= \begin{pmatrix} \xi_1 \\ \vdots \\ \xi_N \end{pmatrix}^T \begin{pmatrix} 2J & -J & \cdots & -J \\ -J & 2J & \cdots & 0 \\ \vdots & & & \vdots \\ -J & \cdots & -J & 2J \end{pmatrix} \begin{pmatrix} \xi_1 \\ \vdots \\ \xi_N \end{pmatrix} \\ &= 2\xi_1^T J\xi_1 - \xi_1^T J\xi_2 - \xi_1^T J\xi_N \\ &\quad - \xi_1^T J\xi_2 + 2\xi_2^T J\xi_2 - \xi_2^T J\xi_3 \\ &\quad \vdots \\ &\quad - \xi_N^T J\xi_1 - \xi_N^T J\xi_{N-1} + 2\xi_N^T J\xi_N \\ &= \xi_1^T J\xi_1 - \xi_1^T J\xi_2 - \xi_2^T J\xi_1 + \xi_2^T J\xi_2 \\ &\quad + \xi_2^T J\xi_2 - \xi_2^T J\xi_3 - \xi_3^T J\xi_2 + \xi_3^T J\xi_3 \\ &\quad \vdots \\ &\quad + \xi_N^T J\xi_N - \xi_N^T J\xi_1 - \xi_1^T J\xi_N + \xi_1^T J\xi_1 \\ &= (\xi_1 - \xi_2)^T J(\xi_1 - \xi_2) \\ &\quad \vdots \\ &\quad + (\xi_N - \xi_1)^T J(\xi_N - \xi_1) \\ &= \sum_{i=\langle N\rangle} (\xi_i - \xi_{i+1})^T J(\xi_i - \xi_{i+1}). \end{aligned}$$

The third claim is again shown by direct manipulation

$$\begin{aligned}&\begin{pmatrix} J(\xi_1 - \xi_N) + J(\xi_1 - \xi_2) \\ J(\xi_2 - \xi_1) + J(\xi_2 - \xi_3) \\ \vdots \\ J(\xi_N - \xi_{N-1}) + J(\xi_N - \xi_1) \end{pmatrix} \\ &= \begin{pmatrix} 2J & -J & \cdots & -J \\ -J & 2J & -J & \cdots \\ \vdots & & & \vdots \\ -J & \cdots & -J & 2J \end{pmatrix} \begin{pmatrix} \xi_1 \\ \xi_2 \\ \vdots \\ \xi_N \end{pmatrix} \\ &= (C \otimes J)\boldsymbol{\xi}. \end{aligned}$$

The last claim follows from the fact that the Kronecker product of two positive definite matrices is positive definite [27]. ■

Proof of Theorem IV.1: Letting

$$\tilde{\mathbf{h}} = \left(\tilde{\mathbf{h}}_1^T, \ldots, \tilde{\mathbf{h}}_N^T\right)^T$$

Lemma IV.1 can be used to write E as

$$E = \frac{1}{2}\tilde{\mathbf{h}}^T \left(I_N \otimes K_g + C \otimes K_f\right)\tilde{\mathbf{h}}.$$

Consider the Lyapunov function candidate

$$V = E + \frac{1}{2}\sum_{i=1}^{N} \dot{\mathbf{h}}_i^T \dot{\mathbf{h}}_i \tag{11}$$

which can be written as

$$V = \frac{1}{2}\tilde{\mathbf{h}}^T(I_N \otimes K_g + C \otimes K_f)\tilde{\mathbf{h}} + \frac{1}{2}\dot{\mathbf{h}}^T\dot{\mathbf{h}}.$$

The time derivative of V is

$$\dot{V} = \dot{\mathbf{h}}^T[(I_N \otimes K_g + C \otimes K_f)\tilde{\mathbf{h}} + \boldsymbol{\nu}]$$

where $\boldsymbol{\nu} = (\boldsymbol{\nu}_1^T, \ldots, \boldsymbol{\nu}_N^T)^T$. Noting that the control law (8) can be written in stacked form as

$$\boldsymbol{\nu} = -(I_N \otimes K_g + C \otimes K_f)\tilde{\mathbf{h}} - (I_N \otimes D_g + C \otimes D_f)\dot{\mathbf{h}} \quad (12)$$

we get that

$$\dot{V} = -\dot{\mathbf{h}}^T(I_N \otimes D_g + C \otimes D_f)\dot{\mathbf{h}}$$

which is negative semidefinite by *Lemma IV.1*.

Consider the set $\Omega = \{(\tilde{\mathbf{h}}, \dot{\mathbf{h}}) \,|\, \dot{V} = 0\}$, and let $\bar{\Omega}$ be the largest invariant set in Ω. On $\bar{\Omega}$ we have $\boldsymbol{\nu} = 0$, which implies from (12) that

$$(I_N \otimes K_g + C \otimes K_f)\tilde{\mathbf{h}} = 0.$$

Since $K_g > 0$ and $K_f \geq 0$, the proof follows from *Lemma IV.1* and LaSalle's invariance principle [28].

The second statement follows by noting that $\dot{V} \leq 0$ implies that $V(t) \leq V(0)$ and

$$E(t) + \sum_{i=1}^{N} \dot{\mathbf{h}}_i^T \dot{\mathbf{h}}_i = 2V(t) \leq 2V(0) = E(0)$$
$$\Rightarrow E(t) \leq E(0) - \sum_{i=1}^{N} \dot{\mathbf{h}}_i^T \dot{\mathbf{h}}_i$$

where the third equality follows from the fact that the formation is initially at rest. ∎

Equation (9) provides a bound on the error function $E(t)$. While the bound is very conservative, it implies that during a maneuver, the error will never be worse than the initial error. It is interesting to note that the bound becomes tighter as the velocity of the robots increase. Hardware results demonstrating the effectiveness of (8) are contained in Section V.

B. Coupled Dynamics Formation Control With Passivity-Based Interrobot Damping

The control strategy given in (8) requires that the relative velocity between neighbors is known. If relative velocity information is not known, then one possible strategy is to set $D_f = 0$. Unfortunately, this choice results in relative motion that is oscillatory, despite smooth transition of each of the individual robots to their desired formation pattern. To eliminate this oscillation, we use passivity techniques [29]–[31] to inject relative damping into the system. The proposed control strategy is given by

$$\begin{aligned}\dot{\hat{\mathbf{x}}}_i &= A\hat{\mathbf{x}}_i + \tilde{\mathbf{h}}_i \\ \boldsymbol{\nu}_i &= -(K_g + P)\tilde{\mathbf{h}}_i - D\dot{\mathbf{h}}_i \\ &\quad - K_f(\tilde{\mathbf{h}}_i - \tilde{\mathbf{h}}_{i-1}) - K_f(\tilde{\mathbf{h}}_i - \tilde{\mathbf{h}}_{i+1}) - PA\hat{\mathbf{x}}_i \quad (13)\end{aligned}$$

where K_g and D are positive definite, K_f is positive semidefinite, A is Hurwitz, and P is the positive definite solution to the Lyapunov equation $A^TP + PA^T = -Q$, where Q is positive definite.

The state of the dynamic controller is $\hat{\mathbf{x}}_i$ and represents, in a sense, the estimate of the relative velocities between neighbors. Note the presence of the robot velocity $\dot{\mathbf{h}}_i$. Since this information is required for feedback linearization, we assume that it is also available to the controller.

Theorem IV.2: If the robot formation (1) is subject to the control strategy defined in (5) and (13), then the error function (7) converges to zero asymptotically.

Furthermore, if the formation is initially at rest, i.e., $\dot{\mathbf{h}}(0) = 0$, and the passivity filter is initialized as

$$\hat{\mathbf{x}}_i(0) = -A^{-1}\tilde{\mathbf{h}}_i(0)$$

then the formation error is bounded by

$$E(t) \leq E(0) - \sum_{i=1}^{N} \dot{\mathbf{h}}_i^T \dot{\mathbf{h}}_i - \sum_{i=1}^{N} \hat{\mathbf{x}}_i^T P \hat{\mathbf{x}}_i. \quad (14)$$

Proof: Defining $\hat{\mathbf{x}} = (\hat{\mathbf{x}}_1^T, \ldots, \hat{\mathbf{x}}_N^T)^T$, and using *Lemma IV.1*, the control strategy (13) can be written as

$$\begin{aligned}\dot{\hat{\mathbf{x}}} &= (I_N \otimes A)\hat{\mathbf{x}} + \tilde{\mathbf{h}} \\ \boldsymbol{\nu} &= -[(I_N \otimes K_g) + (C \otimes K_f) + (I_N \otimes P)]\tilde{\mathbf{h}} \\ &\quad - (I_N \otimes D)\dot{\mathbf{h}} \\ &\quad - (I_N \otimes P)(I_N \otimes A)\hat{\mathbf{x}}.\end{aligned}$$

Consider the Lyapunov function candidate

$$V = \frac{1}{2}\tilde{\mathbf{h}}^T(I_N \otimes K_g + C \otimes K_f)\tilde{\mathbf{h}} + \frac{1}{2}\dot{\mathbf{h}}^T\dot{\mathbf{h}} + \frac{1}{2}\dot{\hat{\mathbf{x}}}(I_N \otimes P)\dot{\hat{\mathbf{x}}}.$$

The time derivative of V is given by

$$\dot{V} = \dot{\mathbf{h}}[(I_N \otimes K_g + C \otimes K_f)\tilde{\mathbf{h}} + \boldsymbol{\nu}] + \frac{1}{2}\ddot{\hat{\mathbf{x}}}(I_N \otimes P)\dot{\hat{\mathbf{x}}} + \frac{1}{2}\dot{\hat{\mathbf{x}}}(I_N \otimes P)\ddot{\hat{\mathbf{x}}}$$

where $\ddot{\mathbf{x}} = (I_N \otimes A)\dot{\mathbf{x}} + \dot{\mathbf{h}}$. Using the fact that $(I_N \otimes P)(I_N \otimes A) + (I_N \otimes A)^T(I_N \otimes P) = -(I_N \otimes Q)$, we get

$$\dot{V} = \dot{\mathbf{h}}[(I_N \otimes K_g + C \otimes K_f + I_N \otimes P)\tilde{\mathbf{h}} + (I_N \otimes P)(I_N \otimes A)\dot{\hat{x}} + \boldsymbol{\nu}] - \dot{\hat{\mathbf{x}}}(I_N \otimes Q)\dot{\hat{\mathbf{x}}}.$$

Application of the control law (13) gives

$$\dot{V} = -\dot{\mathbf{h}}^T D\dot{\mathbf{h}} - \dot{\hat{\mathbf{x}}}(I_N \otimes Q)\dot{\hat{\mathbf{x}}}$$

which is negative semidefinite.

Let $\Omega = \{(\tilde{\mathbf{h}}, \dot{\mathbf{h}}, \dot{\hat{\mathbf{x}}}) \,|\, \dot{V} = 0\}$, and let $\bar{\Omega}$ be the largest invariant set in Ω. On $\bar{\Omega}$, we have $\boldsymbol{\nu} = 0$, therefore, (13) implies that the following two equalities hold:

$$\begin{aligned}&(I_N \otimes A)\hat{\mathbf{x}} + \tilde{\mathbf{h}} = 0 \\ &[(I_N \otimes K_g) + (C \otimes K_f) + (I_N \otimes P)]\tilde{\mathbf{h}} \\ &\quad + (I_N \otimes P)(I_N \otimes A)\hat{\mathbf{x}} = 0.\end{aligned}$$

Combining these two equations gives

$$[(I_N \otimes K_g) + (C \otimes K_f)]\tilde{\mathbf{h}} = 0$$

from which asymptotic stability follows by application of LaSalle's invariance principle.

The second statements follows from the same argument used in *Theorem IV.1*. ■

C. Saturated Control

Our experience is that (8) and (13) work well in the presence of actuator saturation, however, convergence is not necessarily guaranteed. In this section, we derive a coupled dynamics strategy that explicitly accounts for actuator saturation.

The saturation control problem appends the additional constraints $|F| \leq F_{\max}$ and $|\tau| \leq \tau_{\max}$, to the dynamics (1). For the robots used in our testbed, these bounds are $F_{\max} = 30$ N and $\tau_{\max} = 230$ Nm. Unfortunately, force and torque bounds cannot be applied directly to the feedback linearized dynamics (5), since the feedback linearization explicitly depends on the tangential and angular velocity of each robot. However, since each formation maneuver prescribes a finite motion, we can assume, that given the bounded acceleration of the system, the robot velocity will also be bounded, and thereby derive bounds

$$\|\boldsymbol{\nu}\| \leq \nu_{\max}$$

on the feedback linearized forces. The saturation problem is solved by modifying the error function (7) to have linear, rather than quadratic, growth. Accordingly, let

$$E_g = \sum_{i=1}^{N} \left[\frac{1}{k} \log(\cosh(k\tilde{h}_{xi})) + \frac{1}{k} \log(\cosh(k\tilde{h}_{yi})) \right]$$

$$E_f = \sum_{i=\langle N \rangle} \left[\frac{1}{k} \log(\cosh(k(\tilde{h}_{xi} - \tilde{h}_{x,i+1}))) + \frac{1}{k} \log(\cosh(k(\tilde{h}_{yi} - \tilde{h}_{y,i+1}))) \right].$$

Similar to (7), the total error function is defined as

$$E = k_f E_f + k_g E_g. \tag{15}$$

The proposed control strategy is

$$\begin{aligned} \boldsymbol{\nu}_i = &-k_g \tanh(k\tilde{\mathbf{h}}_i) - d \tanh(k\dot{\mathbf{h}}_i) \\ &- k_f \tanh(k(\tilde{\mathbf{h}}_i - \tilde{\mathbf{h}}_{i-1})) \\ &- k_f \tanh((\tilde{\mathbf{h}}_i - \tilde{\mathbf{h}}_{i+1})) \end{aligned} \tag{16}$$

where $k_g, k, d > 0$, and $k_f \geq 0$, and where $\tanh$ is applied element wise. The first two terms move the robot toward the desired formation pattern, and the last two terms cause the robots to move into, and maintain, formation.

Theorem IV.3: If the robot formation (1) is subject to the control strategy defined in (5) and (16), then the control satisfies the saturation constraint

$$\|\boldsymbol{\nu}\|_\infty \leq k_g + d + 2k_f$$

and the error function (15) converges to zero asymptotically.

Furthermore, if the formation is initially at rest, then the formation error (15) satisfies

$$E(t) \leq E(0) - \frac{1}{2} \sum_{i=1}^{N} \dot{\mathbf{h}}_i^T \dot{\mathbf{h}}_i.$$

Proof: Since each component of $\tanh$ is bounded by one, each component of the control law will be bounded by $k_g + d + 2k_f$.

Consider the Lyapunov function candidate

$$V = E + \frac{1}{2} \sum_{i=1}^{N} \dot{\mathbf{h}}_i^T \dot{\mathbf{h}}_i$$

where E is given by (15). Using the fact that $(d/dt)\log(\cosh(\xi)) = \dot{\xi}\tanh(\xi)$, the time derivative of V is given by

$$\dot{V} = k_g \sum_{i=1}^{N} \dot{\mathbf{h}}_i^T \tanh(k\tilde{\mathbf{h}}_i) + k_f \sum_{i=\langle N \rangle} (\dot{\mathbf{h}}_i - \dot{\mathbf{h}}_{i+1})^T \tanh(k(\tilde{\mathbf{h}}_i - \tilde{\mathbf{h}}_{i+1})) + \sum_{i=1}^{N} \dot{\mathbf{h}}_i^T \boldsymbol{\nu}_i$$

which, using the fact that $\tanh$ is an odd function, can be rearranged as

$$\begin{aligned} \dot{V} = \sum_{i=\langle N \rangle} \dot{\mathbf{h}}_i^T [&k_g \tanh(k\tilde{\mathbf{h}}_i) + k_f \tanh(k(\tilde{\mathbf{h}}_i - \tilde{\mathbf{h}}_{i+1})) \\ &+ k_f \tanh(k(\tilde{\mathbf{h}}_i - \tilde{\mathbf{h}}_{i-1})) + \boldsymbol{\nu}_i]. \end{aligned}$$

Substituting from (16), we get

$$\dot{V} = -d \sum_{i=1}^{N} \dot{\mathbf{h}}_i^T \tanh(k\dot{\mathbf{h}}_i)$$

which implies that V is a valid Lyapunov function candidate. Let $\Sigma = \{\tilde{\mathbf{h}}_i, \dot{\mathbf{h}}_i \,|\, \dot{V} = 0\}$, and let $\bar{\Sigma}$ be the largest invariant set contained in Σ. On $\bar{\Sigma}$, we know that $\boldsymbol{\nu} = 0$, which implies that

$$\begin{aligned} k_g \tanh(k\tilde{\mathbf{h}}_i) + k_f \tanh(k(\tilde{\mathbf{h}}_i - \tilde{\mathbf{h}}_{i+1})) \\ + k_f \tanh(k(\tilde{\mathbf{h}}_i - \tilde{\mathbf{h}}_{i-1})) = 0 \end{aligned}$$

which can be written as

$$\begin{aligned} (k_g + 2k_f) &\tanh(k\tilde{\mathbf{h}}_i) \\ &+ k_f(\tanh(k(\tilde{\mathbf{h}}_i - \tilde{\mathbf{h}}_{i+1})) - \tanh(k\tilde{\mathbf{h}}_i)) \\ &+ k_f(\tanh(k(\tilde{\mathbf{h}}_i - \tilde{\mathbf{h}}_{i-1})) - \tanh(k\tilde{\mathbf{h}}_i)) = 0. \end{aligned} \tag{17}$$

We will show that this equation implies that the x component of $\tilde{\mathbf{h}}_i$ is equal to zero. Similar arguments show that the y component is also zero. Apply the identity (see [32])

$$\tanh(u) - \tanh(v) = \frac{\sinh(u - v)}{\cosh(u)\cosh(v)}$$

to the x component of (17) to obtain

$$\begin{aligned} (k_g + 2k_f) &\sinh(k\tilde{h}_{xi}) \\ &- k_f \mathrm{sech}(k(\tilde{h}_{xi} - \tilde{h}_{x,i+1})) \sinh(k\tilde{h}_{x,i+1}) \\ &- k_f \mathrm{sech}(k(\tilde{h}_{xi} - \tilde{h}_{x,i-1})) \sinh(k\tilde{h}_{x,i-1}) = 0 \end{aligned}$$

which may be written in matrix form as

$$((k_g + 2k_f) I_N + B) \begin{pmatrix} \sinh(k\tilde{h}_{x1}) \\ \sinh(k\tilde{h}_{x2}) \\ \vdots \\ \sinh(k\tilde{h}_{xN}) \end{pmatrix} = 0 \tag{18}$$

where

$$B = -k_f \sum_{i=\langle N \rangle} \Big(e_i e_{i+1}^T \operatorname{sech}(k(\tilde{h}_{xi} - \tilde{h}_{x,i+1})) + e_i e_{i-1}^T \operatorname{sech}(k(\tilde{h}_{xi} - \tilde{h}_{x,i-1})) \Big).$$

Since $\sinh(k\tilde{h}_{xi}) = 0$ if and only if $\tilde{h}_{xi} = 0$ to prove that $\tilde{h}_{xi} \to 0$ for all i, it is sufficient to show that $(k_g + 2k_f)I_N + B$ is full rank.

To do this, calculate the induced two-norm $||B||_2$. Letting $w = \sum_{j=1}^{N} w_j e_j$ be an arbitrary nonzero vector, gives

$$\begin{aligned}
&||Bw||_2 \\
&= k_f \left\| \sum_{i=\langle N \rangle} \left(e_i e_{i+1}^T \operatorname{sech}(k(\tilde{h}_{xi} - \tilde{h}_{x,i+1}))w \right. \right. \\
&\quad \left. \left. + \sum_{i=\langle N \rangle} e_i e_{i-1}^T \operatorname{sech}(k(\tilde{h}_{xi} - \tilde{h}_{x,i-1})) \right) w \right\|_2 \\
&\le k_f \left\| \sum_{i=\langle N \rangle} \left(e_i e_{i+1}^T \operatorname{sech}(k(\tilde{h}_{xi} - \tilde{h}_{x,i+1}))w \right\|_2 \right. \\
&\quad \left. + \left\| \sum_{i=\langle N \rangle} e_i e_{i-1}^T \operatorname{sech}(k(\tilde{h}_{xi} - \tilde{h}_{x,i-1})) \right) w \right\|_2 \\
&= k_f \left\| \sum_{i=\langle N \rangle} \sum_{\ell=1}^{N} \left(e_i e_{i+1}^T e_\ell w_\ell \operatorname{sech}(k(\tilde{h}_{xi} - \tilde{h}_{x,i+1})) \right\|_2 \right. \\
&\quad \left. + k_f \left\| \sum_{i=\langle N \rangle} \sum_{\ell=1}^{N} e_i e_{i-1}^T e_\ell w_\ell \operatorname{sech}(k(\tilde{h}_{xi} - \tilde{h}_{x,i-1})) \right) \right\|_2 \\
&= k_f \left\| \sum_{i=\langle N \rangle} \sum_{j=1}^{N} \left(e_i \delta_{i+1,\ell} w_\ell \operatorname{sech}(k(\tilde{h}_{xi} - \tilde{h}_{x,i+1})) \right\|_2 \right. \\
&\quad \left. + k_f \left\| \sum_{i=\langle N \rangle} \sum_{j=1}^{N} e_i \delta_{i-1,\ell} w_\ell \operatorname{sech}(k(\tilde{h}_{xi} - \tilde{h}_{x,i-1})) \right) \right\|_2 \\
&= k_f \left\| \sum_{i=\langle N \rangle} (e_i w_{i+1} \operatorname{sech}(k(\tilde{h}_{xi} - \tilde{h}_{x,i+1})) \right\|_2 \\
&\quad + k_f \left\| \sum_{i=\langle N \rangle} e_i w_{i-1} \operatorname{sech}(k(\tilde{h}_{xi} - \tilde{h}_{x,i-1}))) \right\|_2 \\
&= k_f \sqrt{\sum_{i=\langle N \rangle} w_{i+1}^2 \operatorname{sech}(k(\tilde{h}_{xi} - \tilde{h}_{x,i+1}))^2} \\
&\quad + k_f \sqrt{\sum_{i=\langle N \rangle} w_{i-1}^2 \operatorname{sech}(k(\tilde{h}_{xi} - \tilde{h}_{x,i-1}))^2} \\
&\le k_f \sqrt{\sum_{i=\langle N \rangle} w_{i+1}^2} + k_f \sqrt{\sum_{i=\langle N \rangle} w_{i-1}^2} \\
&= 2k_f ||w||.
\end{aligned}$$

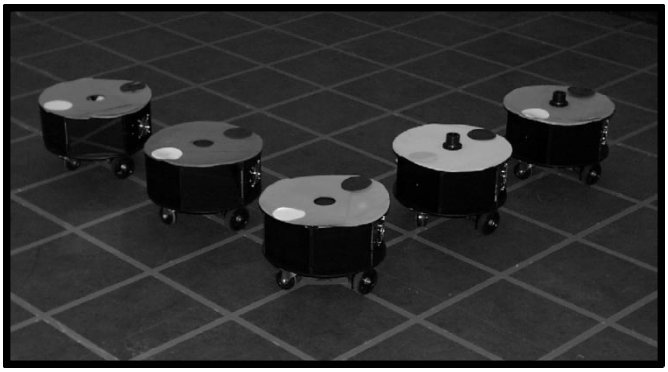

Fig. 3. Robots from the BYU MAGICC laboratory used to obtain experimental results.

TABLE I
PARAMETERS USED TO OBTAIN EXPERIMENTAL RESULTS

Parameter	Value
m_i	$10.1\ kg$
J_i	$0.13\ kg\ m^2$
L_i	$0.12\ m$
K_g Eq. (8)	$0.5I_2$
D_g Eq. (8)	I_2
K_f Eq. (8)	$5I_2$
D_f Eq. (8)	I_2
A Eq. (13)	$-5I_2$
Q Eq. (13)	I_2
K_g Eq. (13)	$10I_2$
D_g Eq. (13)	I_2
K_f Eq. (13)	$5I_2$
k_g Eq. (16)	1
d_g Eq. (16)	5
k_f Eq. (16)	5
k Eq. (16)	1

Since the choice of w was arbitrary, it follows that the induced two-norm satisfies

$$||B||_2 \le 2k_f.$$

Since $(k_g + 2k_f)I_N$ is nonsingular with minimum singular value $\underline{\sigma}((k_g + 2k_f)I_N) = k_g + 2k_f$, and since the maximum singular value of B is $\bar{\sigma} \le 2k_f$, a sufficient condition for $(k_g + 2k_f)I_N + B$ to be full rank is $k_g + 2k_f > 2k_f$, which is always true, since $k_g > 0$. ■

V. HARDWARE RESULTS

This section describes experimental results using the control strategies described in Section IV. Experimental results were obtained on three robots at the Brigham Young University (BYU) MAGICC[1] laboratory which are shown in Fig. 3. The physical parameters of the robots shown in Fig. 3 are listed in Table I.

[1]Multiple AGent Interactive Coordination and Control

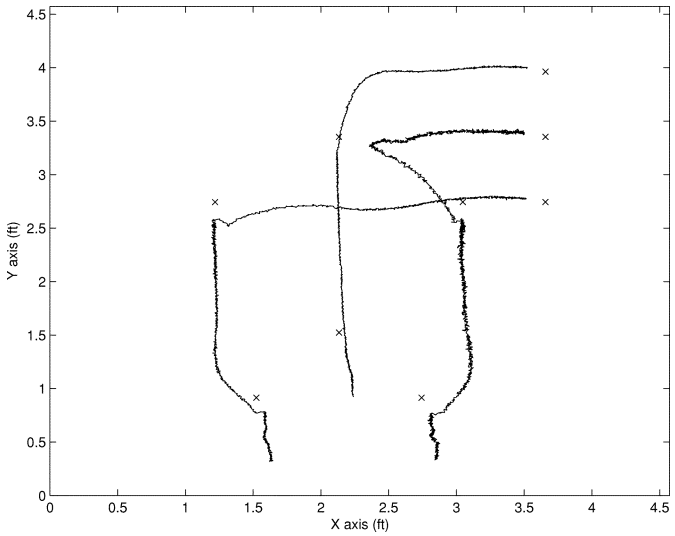

Fig. 4. Robot hand positions for coupled dynamics control strategy (8).

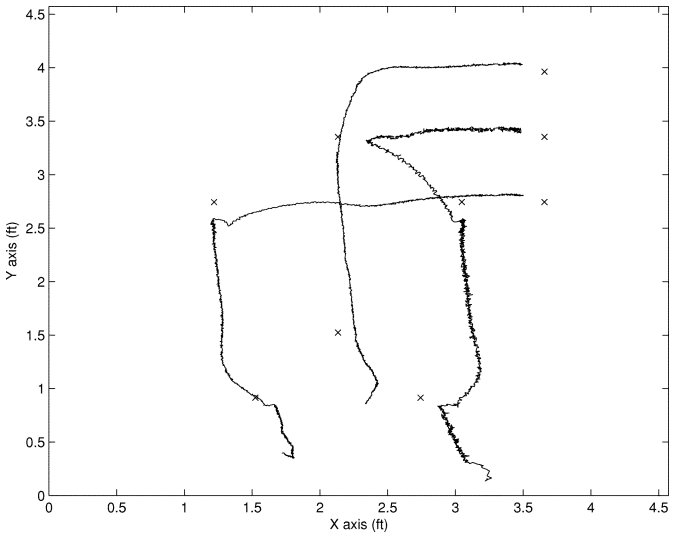

Fig. 5. Robot hand positions for coupled dynamics with passivity control strategy (13).

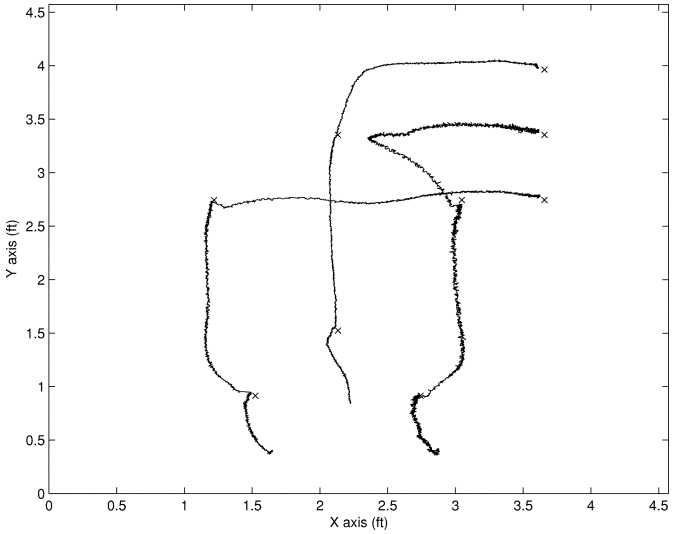

Fig. 6. Robot hand positions for coupled dynamics with input saturation control strategy (16).

The robots are commanded to transition through the series of formation patterns given by

$$\mathcal{P}_1 = \left\{ \begin{pmatrix} 0 \\ -3 \end{pmatrix}, \begin{pmatrix} 1 \\ -4 \end{pmatrix}, \begin{pmatrix} -1 \\ -4 \end{pmatrix} \right\}$$
$$\mathcal{P}_2 = \left\{ \begin{pmatrix} 0 \\ 4 \end{pmatrix}, \begin{pmatrix} 2 \\ 2 \end{pmatrix}, \begin{pmatrix} -2 \\ 2 \end{pmatrix} \right\}$$
$$\mathcal{P}_3 = \left\{ \begin{pmatrix} 5 \\ 6 \end{pmatrix}, \begin{pmatrix} 5 \\ 4.5 \end{pmatrix}, \begin{pmatrix} 5 \\ 3 \end{pmatrix} \right\}$$

where the units are given in feet. The test facility at the BYU MAGICC lab is a 15-foot square. The robots are initially in the formation pattern given by

$$\mathcal{P}_0 = \left\{ \begin{pmatrix} 0 \\ -6 \end{pmatrix}, \begin{pmatrix} 1.5 \\ -6 \end{pmatrix}, \begin{pmatrix} -1.5 \\ -6 \end{pmatrix} \right\}.$$

Fig. 4 shows the robots transitioning between the formation pattern using control strategy (8) and the gains given in Table I. The desired formation patterns are shown by "x" marks. Notice that the robots move into the formation specified by the target formation pattern, at the beginning of each maneuver. The formation maneuver is defined to be complete when $E(t) < \epsilon$. For all of the results shown in this paper, $\epsilon = 0.5$ m. When the formation maneuver is complete, the robots begin to maneuver to the next formation pattern. This accounts for the fact that the robots do not exactly reach the formation patterns shown in Fig. 4.

Fig. 5 shows the robots transitioning between the formation patterns using control strategy (13) and the gains given in Table I.

Fig. 6 shows the robots transitioning between the formation patterns using control strategy (16) and the gains given in Table I. For this experiment, the formation gains have been tuned to cause the robots to move into formation quickly, before transitioning to the desired formation pattern.

VI. Conclusion

In this paper, we have considered the problem of transitioning a group of robots through a sequence of formation patterns. The group objective is to maintain the same formation as the desired formation pattern during the transition. Three control strategies were considered and were shown to meet the formation objectives. Hardware results demonstrate the effectiveness of the proposed strategies.

Acknowledgment

The authors gratefully acknowledge the assistance of J. Kelsey, P. Jones, and M. Blake in obtaining the experimental results.

References

[1] W. C. Dickson, R. H. Cannon, and S. M. Rock, "Symbolic dynamic modeling and analysis of object/robot-team systems with experiments," in *Proc. IEEE Conf. Robotics and Automation*, Minneapolis, MN, Apr. 1996, pp. 1413–1420.

[2] C. R. Kube and H. Zhang, "The use of perceptual cues in multi-robot box-pushing," in *Proc. IEEE Int. Conf. Robotics and Automation*, Minneapolis, MN, Apr. 1996, pp. 2085–2090.
[3] T. Vidal, M. Ghallab, and R. Alami, "Incremental mission allocation to a large team of robots," in *Proc. IEEE Int. Conf. Robots and Automation*, Minneapolis, MN, Apr. 1996, pp. 1620–1625.
[4] D. Kurabayashi, J. Ota, T. Arai, and E. Yoshida, "Cooperative sweeping by multiple mobile robots," in *Proc. IEEE Int. Conf. Robotics and Automation*, Minneapolis, MN, Apr. 1996, pp. 1744–1749.
[5] M. O. Anderson, M. D. Mckay, and B. S. Richardson, "Multirobot automated indoor floor characterization team," in *Proc. IEEE Conf. Robotics and Automation*, Minneapolis, MN, Apr. 1996, pp. 1750–1753.
[6] H. Yamaguchi, "Adaptive formation control for distributed autonomous mobile robot groups," in *Proc. IEEE Int. Conf. Robotics and Automation*, Albuquerque, NM, Apr. 1997, pp. 2300–2305.
[7] P. K. C. Wang, "Navigation strategies for multiple autonomous mobile robots moving in formation," *J. Robot. Syst.*, vol. 8, no. 2, pp. 177–195, 1991.
[8] P. K. C. Wang and F. Y. Hadaegh, "Coordination and control of multiple microspacecraft moving in formation," *J. Astronautical Sci.*, vol. 44, no. 3, pp. 315–355, 1996.
[9] J. P. Desai, J. Ostrowski, and V. Kumar, "Controlling formations of multiple mobile robots," in *Proc. IEEE Int. Conf. Robotics and Automation*, Leuven, Belgium, May 1998, pp. 2864–2869.
[10] M. Mesbahi and F. Y. Hadaegh, "Formation flying control of multiple spacecraft via graphs, matrix inequalities, and switching," *AIAA J. Guidance, Control, Dynam.*, vol. 24, no. 2, pp. 369–377, Mar.–Apr. 2000.
[11] T. Balch and R. C. Arkin, "Behavior-based formation control for multirobot teams," *IEEE Trans. Robot. Automat.*, vol. 14, pp. 926–939, Dec. 1998.
[12] M. Schneider-Fontan and M. J. Mataric, "Territorial multirobot task division," *IEEE Trans. Robot. Automat.*, vol. 14, pp. 815–822, Oct. 1998.
[13] Q. Chen and J. Y. S. Luh, "Coordination and control of a group of small mobile robots," in *Proc. IEEE Int. Conf. Robotics and Automation*, 1994, pp. 2315–2320.
[14] M. Veloso, P. Stone, and K. Han, "The CMUnited-97 robotic soccer team: Perception and multi-agent control," *Robot. Auton. Syst.*, vol. 29, pp. 133–143, 1999.
[15] L. E. Parker, "ALLIANCE: An architecture for fault-tolerant multirobot cooperation," *IEEE Trans. Robot. Automat.*, vol. 14, pp. 220–240, Apr. 1998.
[16] K. Sugihara and I. Suzuki, "Distributed algorithms for formation of geometric patterns with many mobile robots," *J. Robot. Syst.*, vol. 13, no. 3, pp. 127–139, 1996.
[17] R. W. Beard, J. Lawton, and F. Y. Hadaegh, "A feedback architecture for formation control," *IEEE Trans. Control Syst. Technol.*, vol. 9, pp. 777–790, Nov. 2001.
[18] N. E. Leonard and E. Fiorelli, "Virtual leaders, artificial potentials and coordinated control of groups," in *Proc. IEEE Conf. Decision and Control*, Orlando, FL, Dec. 2001, pp. 2968–2973.
[19] W. Kang, N. Xi, and A. Sparks, "Formation control of autonomous agents in 3D workspace," in *Proc. IEEE Int. Conf. Robotics and Automation*, San Francisco, CA, Apr. 2000, pp. 1755–1760.
[20] M. A. Lewis and K.-H. Tan, "High precision formation control of mobile robots using virtual structures," *Auton. Robots*, vol. 4, pp. 387–403, 1997.
[21] R. W. Brockett, "Asymptotic stability and feedback stabilization," in *Differential Geometric Control Theory*, R. S. Millman and H. J. Sussmann, Eds. Cambridge, MA: Birkhaüser, 1983, pp. 181–191.
[22] A. Astolfi, "Exponential stabilization of a wheeled mobile robot via discontinuous control," *ASME J. Dynam. Syst. Meas. Contr.*, vol. 121, no. 1, pp. 121–125, Mar. 1999.
[23] C. C. de Wit and O. J. Sordalen, "Exponential stabilization of mobile robots with nonholonomic constraints," *IEEE Trans. Automat. Control*, vol. 37, pp. 1791–1797, Nov. 1992.
[24] C. Samson, "Time-varying feedback stabilization of car-like wheeled mobile robots," *Int. J. Robot. Res.*, vol. 12, no. 1, pp. 55–64, Feb. 1993.
[25] J.-B. Pomet, B. Thuilot, G. Bastin, and G. Campion, "A hybrid strategy for the feedback stablization of nonholonomic mobile robots," in *Proc. IEEE Int. Conf. Robotics and Automation*, Nice, France, May 1992, pp. 129–134.
[26] A. Isidori, *Nonlinear Control Systems*, 2nd ed. New York: Springer-Verlag, 1989.
[27] A. Graham, *Kronecker Products and Matrix Calculus: With Applications*. New York: Halsted, 1981.
[28] J. P. LaSalle, "Some extensions of Lyapunov's second method," *IRE Trans. Circuit Theory*, vol. CT-7, pp. 520–527, Apr. 1960.
[29] R. Ortega, A. Loria, R. Kelly, and L. Praly, "On passivity-based output feedback global stabilization of Euler-Lagrange systems," *Int. J. Robust and Nonlinear Control*, vol. 5, pp. 313–323, 1995.
[30] F. Lizarralde and J. Wen, "Attitude control without angular velocity measurement: A passivity approach," *IEEE Trans. Automat. Contr.*, vol. 41, pp. 468–472, Mar. 1996.
[31] P. Tsiotras, "Further passivity results for the attitude control problem," *IEEE Trans. Automat. Contr.*, vol. 43, pp. 1597–1600, Nov. 1998.
[32] W. H. Beyer, Ed., *CRC Standard Mathematical Tables*, 27th ed. Boca Raton, FL: CRC, 1984.

Jonathan R. T. Lawton received the Ph.D. degree in electrical engineering in 2000, the M.S. degree in mathematics in 1997, and the B.S. degree in physics in 1994, all from Brigham Young University, Provo, UT.

He is currently with Raytheon Missile Systems, Tucson, AZ. His work at Raytheon has included development of missile guidance algorithms and target state estimation algorithms.

Randal W. Beard (S'91–M'92–SM'03) received the B.S. degree in electrical engineering from the University of Utah, Salt Lake City, in 1991, and the M.S. degree in electrical engineering in 1993, the M.S. degree in mathematics in 1994, and the Ph.D. degree in electrical engineering in 1995, all from Rensselaer Polytechnic Institute, Troy, NY.

Since 1996, he has been with the Electrical and Computer Engineering Department, Brigham Young University, Provo, UT, where he is currently an Associate Professor. In 1997 and 1998, he was a Summer Faculty Fellow at the Jet Propulsion Laboratory, California Institute of Technology, Pasadena, CA. His research interests include coordinated control of multiple vehicle systems and nonlinear and optimal control.

Dr. Beard is a member of AIAA and Tau Beta Pi and is currently an Associate Editor for the IEEE Control Systems Society Conference Editorial Board.

Brett J. Young received the M.S. and B.S. degrees in electrical engineering in 2000 from Brigham Young University, Provo, UT.

He is currently an RF Systems Engineer with Raytheon Missile Systems, Tucson, AZ. His interests include radar and signal processing techniques.